Nuclear Inst. and Methods in Physics Research, A 954 (2020) 161725

Contents lists available at ScienceDirect

Nuclear Inst. and Methods in Physics Research, A

journal homepage: www.elsevier.com/locate/nima

Factors affecting performance of the micro-layered fast-neutron detector

Priyarshini Ghosh *, Wenkai Fu, Mark J. Harrison, Patrick K. Doyle, Jeremy A. Roberts, Douglas S. McGregor

Department of Mechanical and Nuclear Engineering, Kansas State University, Manhattan KS 66506, United States

ABSTRACT

The Micro-Layered Fast-Neutron Detector (MLFD) is a proton-recoil scintillation detector constituting microscale alternating layers of hydrogenous medium and ZnS:Ag. The device employs a peripheral photon detection for maximizing light collection while minimizing gamma-ray background. The layered configuration offers several novel advantages inherently by design, e.g., it overcomes the light-opacity limitation of polycrystalline ZnS, recoil protons have a high probability of reacting with the scintillation grains in their forward-directional path, the design and photomultiplier orientation eliminates the need for extraneous light guides, and minimizes Ĉerenkov generation and collection. The most striking ability of the MLFD is that its efficiency can be scaled higher by simply adding layers and increasing the length, up to 20 cm. Presently, a 40-mm MLFD has an intrinsic detection efficiency of 9.2% for bare ^{252}Cf. Described is a comparison between experimental results and a theoretical model, the respective performances of which differ in high energy regions. The differences in the two models suggest that epoxy in the MLFD contributes to an increased count rate in higher channels.

Contents

1. Research motivation

Idaho National Laboratory recently restarted the Transient REActor Test (TREAT) facility for the development of safer and more efficient fuels. To help regulators determine fuel-failure thresholds, effects of high-power excursions, and consequences of loss-of-coolant accidents [1], the TREAT instrumentation provides stress-testing of nuclear fuels during which quick, high-energy neutron pulses are generated that simulate mild to severe accident conditions [2]. This instrumentation includes the hodoscope for tracking fuel motion, which consists of 334 steel-collimated channels coupled to 'Hornyak buttons' for detecting fast-neutron pulses. To determine the fuel position at any instant during a transient, fast neutrons from fission in the test fuel are detected by the Hornyak buttons [3]. Collimation ensures pixel-imaging of fuel motion. Stress-testing requires statistical precision of fast-neutron count rates, hence maximizing fast-neutron detection efficiency becomes imperative.

The fissile material primarily emits fast neutrons and gamma rays from fission as the detectable forms of radiation. The choice of radiation detector was based upon the nature of background competition, a major portion of which is gamma rays from fission as well as from capture reactions in the test assembly [3]. Therefore, a fast-neutron detector with acceptable gamma-ray rejection capabilities was chosen to be the sensor. Hornyak buttons had been used in the past because of their relatively low sensitivity to gamma rays, thermal neutrons, and overall better efficiency than other fission counters [3]. The Hornyak button contains a slab of a homogeneous mix of polymethyl methacrylate and silver-doped zinc sulfide, bounded on either side by a half-moon of polymethyl methacrylate serving as light guides [3]. However, Hornyak buttons suffer from low fast-neutron detection efficiency, signal-contamination from Ĉerenkov radiation (generated in the Hornyak button light guides), and non-linearity of detector response at large transients. With TREAT restarting, and approximately a hundred Hornyak buttons remaining

* Correspondence to: 3002 Rathbone Hall 1701B Platt St. Manhattan, KS 66506, USA.
E-mail address: pghosh@ksu.edu (P. Ghosh).

https://doi.org/10.1016/j.nima.2018.12.040
Received 27 July 2018; Received in revised form 10 December 2018; Accepted 12 December 2018
Available online 3 January 2019
0168-9002/

in working condition, there is a need for a suitable neutron detection replacement technology. To overcome the drawbacks characteristic of Hornyak buttons, to enable more accurate and reliable data acquisition, and to improve performance, the Micro-Layered Fast-neutron Detector was developed [4,5].

1.1. Device design & fabrication

It is important to detect fast neutrons directly instead of moderating them to thermal neutrons because the original identity of the neutron can be preserved, and thermal neutrons may be a part of the background in the TREAT environment. Fast neutrons can be directly detected using liquid scintillators, ^{4}He-based gas detectors, and plastic scintillators. Hydrogen-based scintillators generally fare better than other detectors in distinguishing fast neutrons from gamma-ray interactions. Inorganic scintillators commonly used for radiation detection, on the other hand, generally have much higher light output than do organic scintillators. An improved device was designed by combining attributes of organic and inorganic materials [6].

Ag-doped ZnS (ZnS:Ag) was chosen as the scintillating material because of its wide band gap and high light yield for heavy, charged particles (50,000 MeV [7]) but a low conversion efficiency for fast electrons [8], thereby allowing for discrimination of heavily-ionizing particles in an intense gamma-ray background. Adding a dopant into the crystal lattice decreases the light-opacity by introducing allowed states in the forbidden band gap region. ZnS:Ag also introduces additional neutron-induced proton flux by a threshold (n,p) reaction with ^{32}S (approximately 32% of the counting rate observed from a ZnS-Lucite mixture [9]), thereby further increasing fast neutron detection rate. In fact, this reaction predominates when the discriminator bias is set beyond 2 MeV neutron energy [3]. However, ZnS:Ag imposes a limitation on its scintillation efficiency: it is difficult to develop a large single crystal of ZnS, which necessitates the use of multi-crystalline layers of the fluor with individual crystal dimensions of about a few microns. Due to scattering of light at the layer interfaces, light transmission rapidly decreases with increasing thickness of the scintillation medium [8]. Polycrystalline ZnS:Ag becomes opaque to its own luminescence for mass thicknesses greater than 25 mg/cm^2 [10]. Yet it is imperative to maximize the scintillation volume in order to increase chances of scintillation. To circumvent this limitation, the scintillation medium was oriented in optically-independent sections. The neutron-converter material was selected to be PMMA due to its high hydrogen-to-carbon ratio (1.3:1), high optical transparency [9], excellent radiation-hardness [11], and exhibits the least autofluorescence among all plastics [12], thus making it the most desirable candidate. The PMMA also acts as a light guide for the scintillation photons.

An alternating layered design would facilitate the inclusion of a larger total amount of scintillating material while simultaneously reducing the probability of light self-absorption by limiting the individual layer thickness. In the past, layered devices have been investigated to achieve a higher gamma-ray discrimination ratio and increase the interaction rate of neutrons [13], but their efficiency has been limited mostly due to the opacity of the scintillation layers [14]. The MLFD has averted this challenge by fabricating microscale layers of ZnS:Ag. The total scintillation volume in a 25.4-mm long Hornyak button is 16.7 mm^3 while in a 25.4-mm MLFD is 30.5 mm^3. The PMMA and ZnS:Ag layer thicknesses were numerically optimized, based on the range of protons in PMMA, the opacity of ZnS:Ag to its own light, and the ZnS:Ag volume necessary to increase chances of scintillation, to be 200 μm and 12 μm, respectively [4]. The MLFD cross-sectional area was chosen to be 8 mm × 3 mm in consideration of commercial silicon photomultiplier (SiPM) dimensions as well as the hodoscope collimator slit aperture [3]. Recoil protons have a higher probability of interacting with ZnS:Ag molecules on their forward-directional path. The layered design also eliminates the need for external light guides by attaching light-collection devices on the longest face of the detector, as shown in Fig. 1. This orientation also greatly reduces Ĉerenkov contamination in two ways: firstly, Ĉerenkov production is reduced by eliminating external light guides. Secondly, Ĉerenkov radiation is still generated in the PMMA layers, which propagates in the direction of the interacting charged particle. Hence, a portion of forward-propagating Ĉerenkov photons is rendered undetectable by the light-detector because light-collection is performed from the side and not from the end. Fig. 2 illustrates the neutron detection and light collection mechanism in the MLFD.

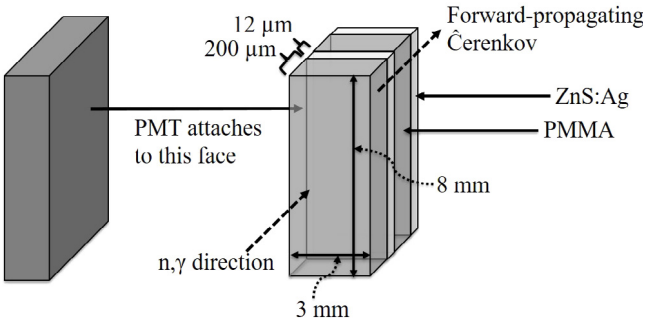

Fig. 1. One of the unique features of the MLFD is that it enables light to be collected from the sides, thereby maximizing light collection and eliminating the need for light guides.

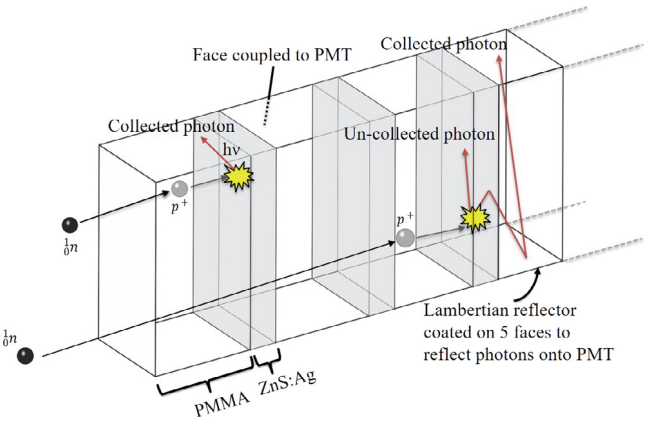

Fig. 2. Neutron detection mechanism in the MLFD.

2. Experimental procedure

The device was fabricated by stacking alternating layers of PMMA and ZnS:Ag. The ZnS:Ag was in powder-form, requiring that it be homogeneously mixed with optically-clear epoxy (90% transmittance at 450 nm) to adhere to the PMMA [5] in a ratio of 40:60 by weight percent, respectively. This ratio was chosen by trial based on attaining a suitably viscous mixture that can be applied smoothly on the surface of the PMMA sheets without forming gaps or air bubbles. Mathematical modeling in Geant4 predicted that increasing the length of the detectors up to 20 cm could maximize detection efficiency [4]. Three lengths of MLFDs were fabricated; a 12-mm, 25.4-mm, and 40-mm MLFD (Fig. 3).

The three MLFD's were optically coupled, separately, to a Hamamatsu R6231 PMT (Fig. 4) in a fashion that emulated the source-detector orientation at TREAT. The MLFD was irradiated with a ^{137}Cs source (166,500 γ/s at the time of the experiment) to determine the Lower Level Discriminator (LLD) setting and to measure its gamma-ray rejection capabilities [5], and with a ^{252}Cf source (40,203 n/s at the time of the experiment) to determine its fast-neutron detection efficiency. ^{252}Cf produces approximately four gamma rays per neutron during its spontaneous fission [15], so a ^{137}Cs source was chosen with an activity closest to the number of gamma rays emitted from the ^{252}Cf source.

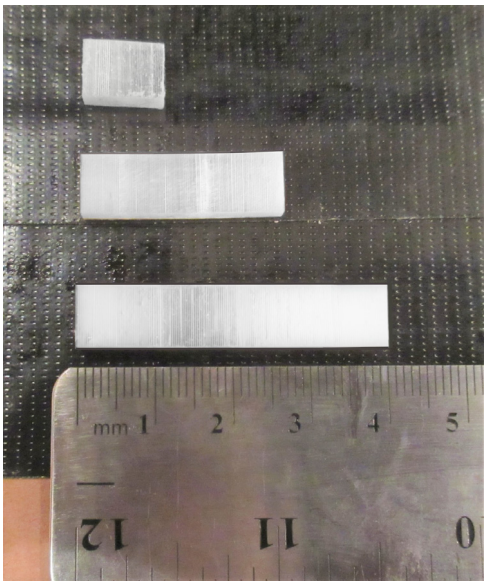

Fig. 3. Three lengths of MLFDs were fabricated and tested: 12 mm, 25.4 mm, 40 mm.

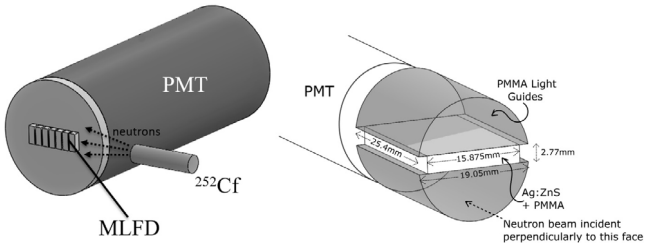

Fig. 4. The detector-source orientation in the experimental setup (left) imitated that of the Hornyak buttons' (right) in the TREAT hodoscope.

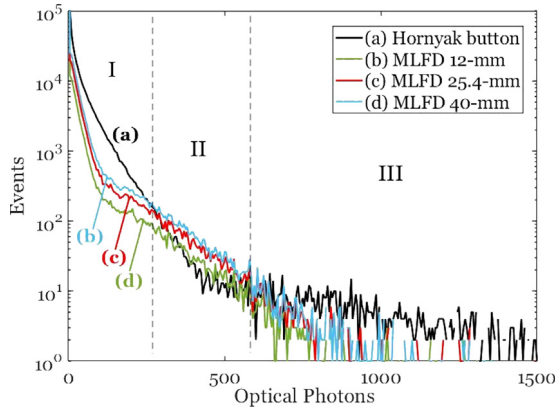

Fig. 5. Theoretical total spectra of the three MLFDs compared to the Hornyak button spectra, on being irradiated with a ^{252}Cf source.

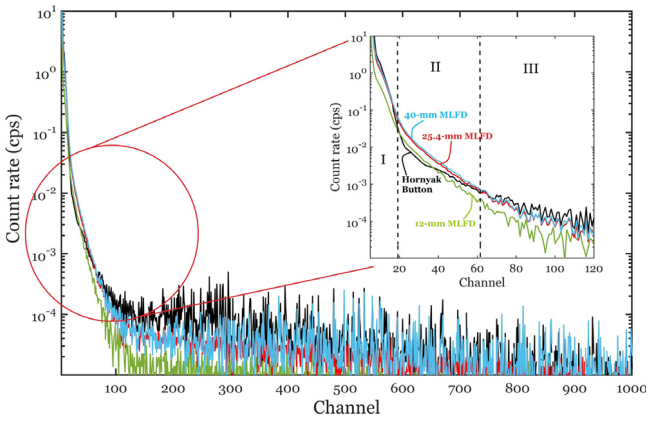

Fig. 6. Experimental spectra of the MLFDs compared to the Hornyak button when irradiated with an unshielded ^{252}Cf source. The inset shows the spectral trends in the initial channels.

2.1. Simulated model

The MLFD was modeled using Geant4 version 10.2 with patch 02. Neutron interactions were performed using the neutron-cross section file G4NDL4.5. Nuclear processes, i.e., neutron and gamma-ray interactions, were simulated using the Geant4 reference QGSP BERT HP physics list. Optical processes (optical absorption, scintillation, Ĉerenkov radiation and boundary interactions) in the G4OpticalPhysics class file were added to the physics list. The detector pulse height was measured in terms of emitted optical photons. Any optical photon reaching the light-collection device was considered 'detected' because of the high PMT photo-detection efficiency from the ZnS(Ag) emission spectrum. The detector response to incident neutrons and gamma rays were computed together to produce a total pulse-height spectrum based on the number of detected optical photons. The ^{252}Cf was modeled as a point source located 10-cm away from the detector parallel to the longest length of the detector, and at the centre of the cross-sectional planes.

The neutron energies were sampled from the Watt fission spectrum for a ^{252}Cf spontaneous fission, sampled by the *R12* sampling algorithm [16]:

$$f(E) \propto \exp\left(-\frac{E}{1.025}\right)\sinh(\sqrt{2.926E}) \text{ [17]}$$

The fission gamma-ray spectrum was defined by the following set of equations [18], sampled by the rejection method:

$$N(E) = \begin{cases} 38.13\,(E-0.085)\,e^{1.648E}, & E < 0.3 \text{ MeV} \\ 26.8e^{-2.30E}, & 0.3 < E < 1.0 \text{ MeV} \\ 8.0e^{-1.1E}, & 1.0 < E < 8.0 \text{ MeV} \end{cases}$$

where *f(E)* and *N(E)* are the number of neutrons and gamma rays of energy E, respectively.

The source particles were emitted isotropically towards the 8-mm × 3-mm face of the MLFD. The source particles were sampled using the G4ParticleGun class, with 10^9 events being sampled for the Hornyak button and the 3 lengths of MLFD each.

3. Results

Shown in Fig. 5 are the theoretical full spectra, including effects from Ĉerenkov generation in the scintillator, gamma rays and neutrons. There are three sections of interest in the spectra: regions I, II and III. Region I depicts an area where count rates from Ĉerenkov and gamma radiation dominate over neutron count rates, especially for the Hornyak button. The steeper slope of the MLFD curve as compared to the Hornyak button depicts the superior gamma-ray rejection capabilities of the former [4]. In region II, the Ĉerenkov contribution is negligible, and the MLFD slope is produced almost exclusively from neutrons [4]. The MLFD count rate is higher than the Hornyak button count rate in region II, owing to the greater volume of scintillation material, higher probability of neutron interaction, and improved light collection in the MLFD. In region III, the MLFD count rates drop slightly below the Hornyak button count rates. The experimental spectra (Fig. 6) has agrees with the predicted spectra in regions I and II, but differ in region III, where the 40-mm MLFD count rate exceed the Hornyak button count rate beyond channel 400. The efficiencies for the 3 lengths are reported in Fig. 7.

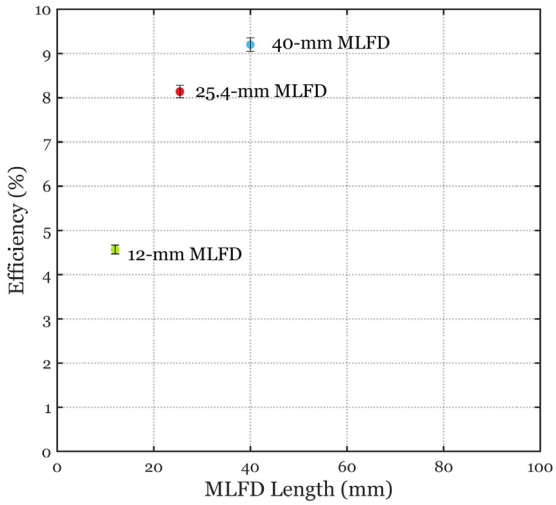

Fig. 7. Intrinsic detection efficiencies for the 3 MLFDs for a bare, isotropic ^{252}Cf source.

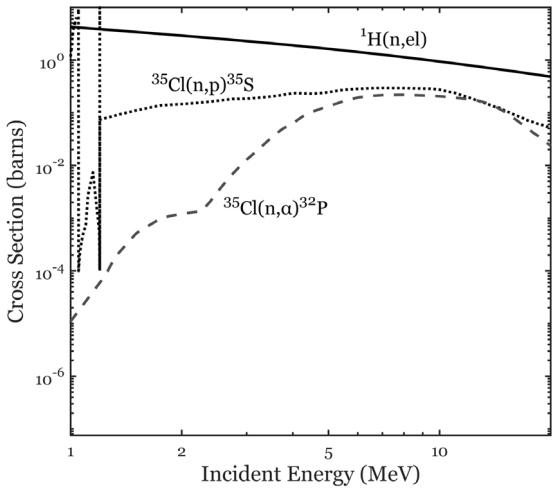

Fig. 8. Neutron cross-sections of reactions from chlorine in the epoxy. For comparison, the main elastic scattering reaction of neutrons with hydrogen is shown [22].

Table 1
Threshold energies for various reactions occurring in the scintillation layer of the MLFD.

Reaction	Q-value	Threshold energy
^{32}S(n, p)^{32}P	−0.93 MeV	0.957 MeV [20]
^{35}Cl(n, p)^{35}S	0.615 MeV	No threshold [21]
^{35}Cl(n, α)^{32}P	0.937 MeV	No threshold [21]

4. Discussion

To explain the disparity between the ideal and fabricated detectors, one must note the key differences between the experimental setup and the theoretical model. The simulation assumed an ideal MLFD, and therefore modeled the scintillator without any epoxy. The fabricated MLFD contains a homogeneously mixed epoxy ($C_{21}H_{25}ClO_5$) and ZnS:Ag in each scintillation layer. The presence of the epoxy in the ZnS:Ag layer reduces the advantage of forward-propagating protons in the ZnS:Ag layer and therefore lowers their probability of interaction. The homogeneous mixture of epoxy and ZnS:Ag consequently also causes lower interaction of forward-propagating Ĉerenkov and gamma rays, a desirable quality. Another effect of the inclusion of the epoxy is the reduction in the total number of layers for any given length of an ideal MLFD, thereby reducing the ZnS:Ag content by 11.2% (by weight). The total amount of hydrogen is reduced very slightly (1.1%) because the H in the epoxy compensates for the missing PMMA layers. This difference will clearly result in reduced scintillation and light collection. On the other hand, the cured epoxy also contains an undetermined amount of chlorine, leading to additional counts by the ^{35}Cl(n,p)^{35}S and ^{35}Cl(n,α)^{32}P reactions (see Table 1), especially beyond 2 MeV (Fig. 8). This phenomenon might explain the slight minor increase in count rates observed at higher channels (Fig. 7). However, the chlorine content is unknown because, while chlorine is a part of a by-product that should have been expelled out of the epoxy upon curing, an appreciable portion of it remains in the cured plastic as hydrolyzable and inactive chlorine [19]. For the initial channels, the lower content of ZnS:Ag, and diminished forward-propagated detection for both neutrons and gamma rays may offset the slight increase in counts due to the aforementioned reactions with chlorine. Additionally, chlorine is known to degrade the optical properties and induce de-lamination over time.

5. Conclusions

The novelty of the MLFD lies in the advantages of using microscale layers of scintillator and neutron-converter, and its light-collection orientation. The device is a multi-layer proton-recoil scintillator that institutes light-collection from the sides, making it easy to achieve very high efficiencies by simply increasing the length of the MLFD. The MLFD is direction-dependent, a feature that is important in reducing cross-talk between detectors in the array as well as in minimizing background radiation from reflected sources. Three lengths of MLFD's were fabricated and their performances compared to theoretical, ideal models. The ideal model contains alternating layers of PMMA and pure ZnS:Ag, but the experimental MLFD had to be fabricated using epoxy to adhere the ZnS:Ag to the PMMA sheets. The spectral trends of both models agreed well in the initial channels, wherein the Ĉerenkov, gamma-ray and neutron count rate trends were accurately predicted by the simulated model. But deviations from the predicted spectra appeared at higher channels, where the devices, especially the 40-mm MLFD, exhibited higher counts than expected. Based on the design deviations, difference in amounts of scintillation material, and differences in theoretical and experimental spectra, it is suspected that it is the epoxy that alters the performance of the detector. Although results indicate that the chlorine in the epoxy may be leading to slightly higher counts for higher energy neutrons, the homogeneous mixture of epoxy with the scintillation material should be detrimental to neutron detection, and beneficial in rejection of gamma rays. To test this hypothesis, a MLFD with lesser or no epoxy content is required, which could also be used to compare with the existing MLFD for any deviations in the lower channels.

Ongoing and future efforts involve fabricating a MLFD with a smaller ratio of epoxy to ZnS:Ag in the scintillation layer. Although the best scenario would be to have zero epoxy, methods of layer deposition such as molecular beam epitaxy and chemical bath deposition would not be able to create an epoxy-less multi-layer system. Chemical bath deposition would also be tedious as each layer would have to be deposited separately, and would introduce additional chemicals into the layer. Pulsed laser deposition (PLD) is another candidate technique that may significantly reduce the epoxy content while controlling the layer thickness more accurately, but will not remove the problem altogether. In fact, PLD will result in a three-alternating layer system: PMMA sheet, deposited ZnS:Ag, and epoxy.

The intrinsic detection efficiency can be scaled higher by increasing the length of the MLFD, although at lengths longer than the 40-mm MLFD, PMTs start to become unfeasible and instead must be replaced with SiPMs. The MLFDs are compact, inexpensive to fabricate and mass-produce, and the goal is to test these new sensors at TREAT to assess their performance in observing fuel motion.

Acknowledgements

This work was supported in part by the U.S. Department of Energy under contract DE-NE0008305. The research and development of the MLFDs was conducted at the Kansas State University Semiconductor Materials and Radiological Technologies (S.M.A.R.T.) Laboratory (Manhattan, KS). The authors would like to thank Dr. David L. Chichester for providing a Hornyak button for testing, and Dr. Amy R. Betz and the Multiphase Microfluidics Laboratory for use of the Minitech Machinery micro-miller.

References

[1] C.E. Dickerman, Studies of fast reactor core behavior under accident conditions, Nucl. Saf. USER 11 (1970) 195–205.
[2] Resumption of transient testing, 2013, (online). https://www.energy.gov/ne/articles/resumption-transient-testing.
[3] A. de Volpi, R.J. Pecina, R.T. Daly, D.J. Travis, R.R. Stewart, E.A. Rhodes, Fast-neutron hodoscope at TREAT: development and operation, Nucl. Technol. 27 (3) (1975) 449–487.
[4] W. Fu, P. Ghosh, M.J. Harrison, D.S. McGregor, J.A. Roberts, A Geant4 evaluation of the Hornyak button and two candidate detectors for the TREAT hodoscope, Nucl. Inst. Methods Phys. Res. A 889 (2018) 39–46.
[5] P. Ghosh, et al., A high-efficiency, low-Ĉerenkov Micro-Layered Fast-Neutron Detector for the TREAT hodoscope, Nucl. Inst. Methods Phys. Res. A 904 (2018) 100–106.
[6] J.A. Roberts, M.J. Harrison, W. Fu, P. Ghosh, D.S. McGregor, Fast-neutron detector developments for the TREAT hodoscope, Radiat. Phys. Chem. (2018).
[7] D.S. McGregor, Materials for gamma-ray spectrometers: inorganic scintillators, Ann. Rev. Mater. Res. 48 (2018) 13.1–13.33.
[8] S.S. Kapoor, V.S. Ramamurthy, Nuclear Radiation Detectors, Wiley Eastern Ltd., New Delhi, India, 1986.
[9] J.B. Birks, The Theory and Practice of Scintillation Counting, First, Pergamon Press, Great Britain, 1964.
[10] S.K. Lee, et al., Comparison of new simple methods in fabricating ZnS(Ag) scintillators for detecting alpha particles, Nucl. Sci. Technol. 1 (2011) 194–197.
[11] Y. Nishiwaki, T. Tsuruta, K. Yamazaki, Detection of fast neutrons by etch-pit method of nuclear track registration in plastics, J. Nucl. Sci. Technol. 8 (3) (1971) 162–166.
[12] A. Piruska, et al., The autofluorescence of plastic materials and chips measured under laser irradiation, Lab Chip 5 (12) (2005) 1348–1354.
[13] M.J. Urffer, Design of a Neutron Detector Capable of Replacing He-3 Detectors Utilizing Thin Polymeric Films, The University of Tennessee, Knoxville, 2012.
[14] J.N. Abdurashitov, et al., A high resolution, low background fast neutron spectrometer, Nucl. Instruments Methods Phys. Res. A 476 (2002) 318–321.
[15] S. Bastola, Spontaneous Fission Spectrum of Neutrons from 252Cf with Kinetic Energies Less than 1 MeV, Brigham Young University, 2012.
[16] D.E. Cullen, Sampling ENDL Watt Fission Spectra, Livermore, CA, US, 2004.
[17] M. Meshkian, Monte Carlo simulation of a fast neutron counter for use in neutron radiography, Nucl. Inst. Methods Phys. Res. A 788 (2015) 73–78.
[18] M. Verbeke, C. Hagmann, D. Wright, Simulation of Neutron and Gamma Ray Emission from Fission and Photofission, Lawrence Livermore Natl. Lab, 2010, pp. 1–30.
[19] W.J. Belanger, S.A. Schulte, Chlorine content of epoxy resins: how it affects the electrical and physical properties of the cured material, Mod. Plast. 37 (3) (1959) 154–159.
[20] J.E. Turner, Atoms, Radiation, and Radiation Protection, third, Compl ed., Wiley-VCH, 2007.
[21] C. Allwork, S. Pitts, Z. Wang, C.L. Morris, Neutron Efficiency and gamma rejection performance of CLYC and 3 He alternative technologies, in: 2015 IEEE Nuclear Science Symposium and Medical Imaging Conference, NSS/MIC, 2015.
[22] Database NEA N ENDF/B-VII.1.